Clinical and Molecular Features of Long-term Response to Immune Checkpoint Inhibitors in Patients with Advanced Non–Small Cell Lung Cancer

Rohit Thummalapalli[1], Biagio Ricciuti[2], Chaitanya Bandlamudi[3], Daniel Muldoon[3], Hira Rizvi[1], Arielle Elkrief[1], Jia Luo[2], Joao V. Alessi[2], Federica Pecci[2], Giuseppe Lamberti[2], Alessandro Di Federico[2], Lingzhi Hong[4], Jianjun Zhang[4], John V. Heymach[4], Don L. Gibbons[4], Andrew J. Plodkowski[5], Vignesh Ravichandran[6], Mark T.A. Donoghue[6], Chad Vanderbilt[3], Marc Ladanyi[3], Charles M. Rudin[1], Mark G. Kris[1], Gregory J. Riely[1], Jamie E. Chaft[1], Matthew D. Hellmann[1], Natalie I. Vokes[4], Mark M. Awad[2], and Adam J. Schoenfeld[1]

ABSTRACT

Purpose: We sought to identify features of patients with advanced non–small cell lung cancer (NSCLC) who achieve long-term response (LTR) to immune checkpoint inhibitors (ICI), and how these might differ from features predictive of short-term response (STR).

Experimental Design: We performed a multicenter retrospective analysis of patients with advanced NSCLC treated with ICIs between 2011 and 2022. LTR and STR were defined as response ≥ 24 months and response < 12 months, respectively. Tumor programmed death ligand 1 (PD-L1) expression, tumor mutational burden (TMB), next-generation sequencing (NGS), and whole-exome sequencing (WES) data were analyzed to identify characteristics enriched in patients achieving LTR compared with STR and non-LTR.

Results: Among 3,118 patients, 8% achieved LTR and 7% achieved STR, with 5-year overall survival (OS) of 81% and 18% among LTR and STR patients, respectively. High TMB (≥50th percentile) enriched for LTR compared with STR ($P = 0.001$) and non-LTR ($P < 0.001$). Whereas PD-L1 ≥ 50% enriched for LTR compared with non-LTR ($P < 0.001$), PD-L1 ≥ 50% did not enrich for LTR compared with STR ($P = 0.181$). Nonsquamous histology ($P = 0.040$) and increasing depth of response [median best overall response (BOR) −65% vs. −46%, $P < 0.001$] also associated with LTR compared with STR; no individual genomic alterations were uniquely enriched among LTR patients.

Conclusions: Among patients with advanced NSCLC treated with ICIs, distinct features including high TMB, nonsquamous histology, and depth of radiographic improvement distinguish patients poised to achieve LTR compared with initial response followed by progression, whereas high PD-L1 does not.

Introduction

Immune checkpoint inhibitors (ICI), including anti–programmed cell death protein 1 (anti–PD-1; refs. 1–3), anti–programmed death ligand 1 (anti–PD-L1; ref. 4), and anti-cytotoxic T-lymphocyte associated protein 4 (anti–CTLA-4; ref. 5) agents, can lead to responses of unprecedented duration in subsets of patients with advanced NSCLC (6, 7), and the prospect of long-term durable responses represents a distinctive benefit of these therapies. Nevertheless, most patients either do not respond to ICIs or develop resistance within 12 to 24 months of an initial response (8–10). Identification of clinical and molecular predictors of long-term ICI benefit among patients with advanced NSCLC is therefore of critical importance to isolate patients who may be poised for durable responses to ICIs without upfront treatment intensification with chemotherapy or other approaches.

Tumor PD-L1 IHC remains the only NSCLC-specific test to determine candidacy for first-line ICI therapy in patients with advanced NSCLC, with patients with PD-L1 ≥ 50% eligible for pembrolizumab (1) and patients with PD-L1 ≥ 1% eligible for combination ipilimumab and nivolumab (5) and pembrolizumab (11). Pembrolizumab is also approved for advanced solid tumors across histologies with tumor mutational burden (TMB) ≥ 10 mutations/megabase (mut/Mb; ref. 12). Whereas markers of response and initial clinical benefit to ICIs in advanced NSCLC have been established, including high TMB (13–16), composites of high TMB and high PD-L1 (17), and tumor-infiltrating lymphocyte (TIL) density (18, 19), whether biomarkers of initial ICI response can reliably distinguish patients poised to achieve a long-term response (LTR) as opposed to a short-term response (STR) has remained unclear. In particular, whether PD-L1 or TMB serve as reliable biomarkers for LTR to ICIs remains uncertain, and have previously only been explored in small studies (20, 21). Among patients with NSCLC treated with ICIs, higher TMB has recently been linked to durable responses (22), while no other immunogenomic or transcriptomic features have been shown to reliably distinguish longer from shorter responses (21). However,

[1]Department of Medicine, Memorial Sloan Kettering Cancer Center, New York, New York. [2]Lowe Center for Thoracic Oncology, Dana-Farber Cancer Institute, Boston, Massachusetts. [3]Department of Pathology and Laboratory Medicine, Memorial Sloan Kettering Cancer Center, New York, New York. [4]Department of Thoracic/Head and Neck Medical Oncology, MD Anderson Cancer Center, Houston, Texas. [5]Department of Radiology, Memorial Sloan Kettering Cancer Center, New York, New York. [6]Marie-Josée and Henry R. Kravis Center for Molecular Oncology, Memorial Sloan Kettering Cancer Center, New York, New York.

R. Thummalapalli and B. Ricciuti are co-first authors.

N.I. Vokes, M.M. Awad, and A.J. Schoenfeld are co-senior authors.

Corresponding Author: Adam J. Schoenfeld, Department of Medicine, Memorial Sloan Kettering Cancer Center, 1275 York Avenue, New York, NY 10065. E-mail: schoenfa@mskcc.org

Clin Cancer Res 2023;29:4408–18

doi: 10.1158/1078-0432.CCR-23-1207

Translational Relevance

Whereas features predictive of initial response to immune checkpoint inhibitors (ICI) in advanced non–small cell lung cancer (NSCLC) have been established, features predictive of long-term response (LTR) remain incompletely understood and require dedicated investigation. Here, in a multicenter cohort of patients with advanced NSCLC treated with ICIs, we identify an 8% frequency of LTR (response ≥ 24 months), with LTR associated with > 80% 5-year survival. We show that high total, clonal, and subclonal tumor mutational burden and distinct clinical features can distinguish patients achieving LTR from patients achieving short-term response (STR: response < 12 months). In contrast, neither high programmed death ligand 1 nor any individual genomic alteration distinguish LTR compared with STR patients. Our results suggest that features predictive of LTR may be distinct from those predictive of initial response, and identify features of patients poised for long-lasting responses to ICIs without upfront treatment intensification.

these observations require validation in larger clinical cohorts. Features predictive of long-term ICI benefit remain incompletely characterized largely due to the general rarity of long-term responders and long durations of follow up required for identification. In addition, the frequency, predictive clinical features, and long-term outcomes of patients with NSCLC achieving LTR to ICIs remain incompletely defined.

In this study, we interrogated a large cohort of advanced patients NSCLC patients treated with ICIs at three academic medical centers to identify the frequency, outcomes, and clinical and immunogenomic features of long-term responders compared with short-term responders, non–long-term responders, and nonresponders to ICIs. Our results help further our understanding of unique predictors of long-term benefit to ICIs in patients with NSCLC and suggest that these may be distinct from those predicting initial response.

Materials and Methods

Patients and efficacy analyses

Patients with advanced (recurrent or metastatic) NSCLC treated with anti–PD-(L)1 monotherapy (ICI monotherapy) or in combination with anti–CTLA-4 therapy (dual ICI therapy) at Memorial Sloan Kettering Cancer Center (MSK) between 2011 and 2020, Dana-Farber Cancer Institute (DFCI, Boston, MA) between 2011 and 2022, and MD Anderson Cancer Center (MDACC) between 2015 and 2019 were included. Patients receiving ICI in combination with chemotherapy or other systemic therapies were excluded. Response Evaluation Criteria in Solid Tumors (RECIST) v1.1 (23) was used to assess efficacy; patients who were not evaluable radiographically were excluded. Progression-free survival (PFS) was defined as the date of anti–PD-(L)1 therapy start to the date of progression. Overall survival (OS) was defined as the date of therapy start to the date of death; patients who did not die were censored at the date of last contact. Patients who had not progressed were censored at the date of their last contact; cases retrospectively adjudicated to not be progressive disease (PD) per RECIST but determined in real-time by the clinician as PD were considered progression events. Best overall response (BOR) was defined as the best RECIST response recorded from the start of therapy until disease progression or death. Categories of BOR included PD, stable disease (SD), partial response (PR), and complete response (CR) per RECIST v1.1 (23). Time on treatment was defined by the date of therapy start to the last date of ICI therapy. Data were collected until July 8, 2022 (MSK), September 28, 2022 (DFCI), and September 1, 2020 (MDACC), when each dataset was locked for outcome analysis. This study was approved by the Institutional Review Board/Privacy Board at MSK and was in accordance with the Belmont report for retrospective review of records and waiver of consent.

Patient cohorts

Patients were divided into the following cohorts for analysis: LTR, STR, PD, and non-LTR. LTR was defined as PR or CR lasting ≥ 24 months from the start of therapy. STR was defined as achievement of PR or CR followed by progression of disease < 12 months from the start of therapy. PD patients were defined as patients with a best response of progressive disease. Non-LTR patients included all patients in each cohort who were not defined as an LTR.

PD-L1 testing

PD-L1 expression was determined on the basis of percentage of tumor cells expressing PD-L1. Subgroups of tumor PD-L1 ≥ 50% and PD-L1 ≥ 90% were used in the analyses. PD-L1 antibodies used in the analyses are detailed in Supplementary Table S1.

Derived neutrophil-to-lymphocyte ratio testing

The results of pretreatment peripheral blood–derived neutrophil—lymphocyte ratio (dNLR) were obtained from subsets of patients. dNLR was defined by [absolute neutrophil count (ANC)]/[total white blood cell count (WBC) – ANC].

Next-generation sequencing analyses and TMB harmonization

The results of next-generation sequencing (NGS) testing obtained prior to the start of ICI therapy were obtained for a subset of patients from MSK and DFCI (n = 1,715 total). Patients from MSK had MSK-IMPACT NGS profiling completed as described below (24), and patients from DFCI had DFCI OncoPanel NGS profiling completed as described below (25, 26).

MSK-IMPACT NGS

Briefly, genomic DNA was extracted from patient tumors and matched normal DNA from peripheral blood samples. Barcoded libraries were generated and sequenced, targeting all exons and select introns of a custom panel of 341 (version 1), 410 (version 2), or 468 (version 3) genes. Mean sequencing coverage across all tumor samples was 750×, with minimum depth of coverage of 38×. Somatic substitutions, small insertions/deletions, gene-level focal copy-number amplifications, homozygous deletions, and fusions in select genes were identified using a clinically validated pipeline (24). To normalize somatic nonsynonymous TMB across panels of various sizes among MSK-IMPACT patients, the total number of nonsynonymous mutations was divided by the coding region captured in each panel, which covered 0.98, 1.06, and 1.22 megabases (Mb) in the 341-, 410-, and 468-gene panels, respectively.

Among MSK-IMPACT patients, the fraction of genome altered (FGA) and whole-genome doubling (WGD) status were inferred from allele-specific copy-number estimates using the FACETS algorithm (27, 28). FGA was defined as the fraction of the genome that is nondiploid; a tumor was considered to have undergone WGD if the fraction of the autosomal genome that has the more frequent allele (major copy number) had a copy number of two or higher (facets-suite v2.0.6 package, https://github.com/mskcc/facets-suite).

HLA genotypes were inferred using Polysolver (ref. 29; RRID: SCR_022278). HLA LOH was determined by the LOHHLA tool (RRID: SCR_023690) as previously described (30) and defined as an allelic imbalance $P < 0.001$ and an estimated raw copy number of HLA allele 1 or allele 2 < 0.5. HLA diversity was defined as the number of unique HLA class I alleles at high resolution (e.g., HLA-A*01:01) within a given sample.

DFCI OncoPanel NGS

Briefly, tumor DNA was extracted and used for custom-designed hybrid capture library preparation. NGS was performed and somatic alterations identified by custom pipeline. Given the absence of matched normal tissue, common SNPs were filtered if present at >0.1% in Exome Variant Server, NHLBI GO Exome Sequencing Project (RRID: SCR_012761), or the Genome Aggregation Database (RRID: SCR_014964); variants present ≥ 2 times in Catalogue Of Somatic Mutations In Cancer (RRID: SCR_002260) were rescued. To minimize inadvertent inclusion of germline variants, consistent with previous aggregation efforts (31), an additional germline filter was applied to exclude events present in the Exome Aggregation Consortium with an allele count > 10, after rescuing known somatic events. TMB was uniformly calculated for each sample as the number of nonsynonymous mutations per Mb of genome covered. DFCI mutation counts were divided by the number of bases covered in each OncoPanel version: v1, 0.75 Mb; v2, 0.83 Mb; and v3, 1.32 Mb. Copy-number variants and structural variants were called using the internally developed algorithms RobustCNV and BreaKmer. For each gene, the absolute copy number (ACN) was estimated on the basis of the tumor purity and the weighted average of segmented $\log_2$ ratios across the gene (l) using the formula $ACN = [2^{(l+1)} - 2(1 - p)]/p$. To quantify aneuploidy levels, targeted sequencing data were analyzed using arm-level somatic copy-number events in targeted sequencing.

TMB harmonization

To facilitate pooled TMB analyses across NGS platforms, harmonized TMB z-scores were calculated as previously described (32). TMB z-score cut-off points included TMB z-score ≥ 0, corresponding to ≥ 50th percentile of TMB in each cohort (≥ 7.9 mut/Mb for MSK, ≥ 10.6 mut/Mb for DFCI), given rough correspondence to the widely used clinical cutoff of TMB ≥ 10 mut/Mb (12), and TMB z-score ≥ 1.16, corresponding to ≥ 90th percentile of TMB in each cohort. To facilitate genomic analyses across platforms, analysis was restricted to oncogenic or likely oncogenic variants as reported by OncoKB (ref. 33; RRID: SCR_014782) and limited to a list of 301 genes included in each version of both NGS platforms (Supplementary Table S2).

Whole-exome sequencing

A subset of 83 patients from MSK (28 LTR, 13 STR, and 42 PD) had tumor and normal tissue profiled by whole-exome sequencing (WES). Enriched exome libraries were sequenced on a HiSeq platform (Illumina) to generate paired-end reads (2 × 76 base pairs) to a target of 150× mean coverage. The mean target coverage was 232× in tumor and 125× in normal sequences; mean target coverage < 60× in tumor or < 30× in normal sequences were excluded. Exomes were processed and analyzed using TEMPO pipeline v1.3 (https://github.com/mskcc/tempo). Briefly, FASTQ files were aligned to human genome reference b37 assembly from the Genome Analysis Toolkit (ref. 34; GATK; RRID: SCR_001876) using BWA mem (v0.7.17; RRID: SCR_010910). Binary alignment map files were sorted using SAMTOOLS v1.9 (RRID: SCR_002105) and marked for PCR duplicates using GATK MarkDuplicates (v3.8–1). Somatic mutations including substitutions and small indels were called in tumor-normal pairs using MuTect2 (v4.1.0.0; RRID: SCR_000559) and Strekla2 (v2.9.10). Somatic mutations were then filtered using the following criteria. First, all variants annotated as oncogenic and likely oncogenic by OncoKB (33) were whitelisted. Then, all nonwhitelisted variants were filtered to exclude those observed in repetitive or low-complexity regions annotated by ENCODE consortium (RRID: SCR_006793; https://hgdownload.cse.ucsc.edu/goldenPath/hg19/database/rmsk.txt.gz and https://genome.ucsc.edu/cgi-bin/hgFileUi?db=hg19&g=wgEncodeMapability). Mutations observed in 10 or more noncancer patients in gnomAD (35) or those with low variant allele frequency (<5%) and supported by three or fewer reads in regions with low coverage (<20×) were filtered out.

Allele-specific copy-number estimates were inferred using FACETS v0.5.6. Clonality of all somatic mutations was inferred using FACETS as described previously (36). Briefly, mutations were deemed clonal if the fraction of cancer cells estimated to have the mutation (cancer cell fraction; CCF) was > 0.8 or if the CCF was > 0.7 and the upper bound of the 95th percentile confidence interval (CI) was > 0.9 (facets-suite v2.0.6 package, https://github.com/mskcc/facets-suite). All other mutations with estimable CCF were deemed subclonal. To estimate TMB, only nonsynonymous mutations within the 25.9 Mb of the coding sequence captured in all tumors sequenced were considered. Clonal and subclonal TMB estimates only considered clonal and subclonal mutations, respectively, as inferred above. Neoantigen peptide–binding affinity predictions were obtained using NetMHCpan-4.1b for all 8 to 11 mer peptides spanning each nonsynonymous mutation (37). Peptides with predicted binding affinities < 500 nm and rank 2% or lower were considered as binders.

Statistical analyses

Mann–Whitney *U* tests were used to complete two-group comparisons of continuous variables, and Fisher exact test was used to compare proportions. Kaplan–Meier methodologies were used to estimate PFS and OS among patient groups. To assess associations of binary clinical covariates with binary clinical outcomes, univariable analyses were completed using Fisher exact test to calculate odds ratios (OR), and multivariable analyses were completed using multiple logistic regression to calculate adjusted ORs. Unbiased analyses of enrichment in frequency of altered genes between groups of clinical outcomes were completed using Fisher exact tests, with multiple hypothesis-corrected adjusted *P* values (P_{adj}) calculated for each gene based on the number of genes tested in a given comparison. For analysis of HLA diversity, the proportion of patients with six unique HLA class I alleles was compared among patient groups. For analyses of WES features, continuous biomarkers were converted to standard z-scores and univariable logistic regression was used to test associations with binary clinical outcomes. All reported *P* values are two-sided, and $P < 0.05$ was considered statistically significant. All statistical analyses were performed with GraphPad Prism v9 (RRID:SCR_002798) and R version 4.2.2 software (RRID: SCR_001905).

Data availability statement

The data generated in this study are available upon request from the corresponding author.

Results

Frequency and clinical outcomes of LTR and STR patients

3,118 patients (MSK: 1469, DFCI: 1183, MDACC: 466) were identified and included in the analysis. Demographic and clinical features of the patient cohorts are described in **Table 1**.

Table 1. Patient characteristics.

Patient characteristics	MSK (no, %)	DFCI (no, %)	MDACC (no, %)	Combined cohort (no, %)
No. of patients (total)	1,469	1,183	466	3,118
Median age, years (range)	68 (22–93)	67 (25–98)	66 (28–91)	67 (22–98)
Sex				
Male	713 (49)	548 (46)	263 (56)	1,524 (49)
Female	756 (51)	635 (54)	203 (44)	1,594 (51)
Smoking status				
Ever (current or former)	1,259 (86)	1,002 (85)	376 (84)	2,637 (85)
Never	210 (14)	181 (15)	90 (16)	481 (15)
ECOG PS at anti–PD-(L)1 initiation				
0	234 (16)	194 (17)	61 (21)	489 (17)
1	1,085 (74)	717 (62)	172 (60)	1,974 (68)
2+	150 (10)	253 (22)	52 (18)	455 (16)
Not available	0	19	181	200
dNLR				
<3.0	864 (59)	476 (59)	263 (77)	1,603 (61)
≥3.0	595 (41)	333 (41)	77 (23)	1,005 (39)
Not available	10	374	126	510
Histology				
Adenocarcinoma	1,110 (76)	918 (78)	352 (76)	2,380 (76)
Squamous cell carcinoma	247 (17)	178 (15)	84 (18)	509 (16)
Other	112 (8)	87 (7)	30 (6)	229 (7)
PD-L1				
<1%	327 (38)	160 (19)	89 (29)	576 (29)
1–49%	184 (21)	249 (30)	94 (30)	527 (26)
≥50%	356 (41)	421 (51)	128 (41)	905 (45)
Not available	602	353	155	1,110
Line of therapy				
1	511 (35)	451 (38)	197 (42)	1,159 (37)
2	666 (45)	507 (43)	215 (46)	1,388 (45)
3+	292 (20)	225 (19)	54 (12)	571 (18)
Anti–PD-(L)1 treatment regimen				
Anti–PD-(L)1 monotherapy	1,332 (91)	1,135 (96)	465 (100)	2,932 (94)
Anti–PD-(L)1 + anti–CTLA-4 therapy	137 (9)	48 (4)	1 (0)	186 (6)
Treatment setting				
Clinical trial	300 (20)	122 (10)	7 (12)	429 (16)
Standard of care	1,169 (80)	1,060 (90)	50 (88)	2,279 (84)
Not available	0	1	409	410

The overall response rate (ORR) among evaluable patients was 21% (95% CI, 19%–22%; **Fig. 1A**), with a 2.0% rate of CR (95% CI, 1.5%–2.6%) and 19% rate of PR (95% CI, 18%–20%). Among all patients, a total of 252 (8%; 95% CI, 7%–9%) achieved LTR (**Fig. 1A**), with similar rates from each site (MSK: 9%, DFCI: 7%, MDACC: 8%; Supplementary Fig. S1A–S1C). STR occurred in 209 patients overall (7%; 95% CI, 6%–8%), with similar rates from each site. Among patients who achieved LTR, the median OS from the start of ICI therapy was not reached during a median follow-up of 55 months; the 5-year OS rate was 81% and the 5-year PFS rate was 57% among patients with LTR (**Fig. 1B**; Supplementary Fig. S2). Among patients with STR, the median OS was 19.3 months, and the 5-year OS rate was 18% (**Fig. 1B**). OS outcomes among LTR, STR, and PD patients were generally concordant across each site (Supplementary Fig. S3A–S3C). The median time on ICI treatment among LTR patients was 25 months, with similar durations across sites (Supplementary Fig. S4A–S4C). The median OS in the entire patient cohort was 13.0 months. Among CRs, the median OS was not reached with a median follow-up duration of 60.5 months, and the 5-year OS rate was 82%. The median PFS among CRs was 59.7 months, with a 5-year PFS rate of 50% (Supplementary Fig. S5A and S5B).

Clinical characteristics of LTR and STR patients

We next aimed to determine clinical characteristics associated with patients who achieved LTR compared with STR, non-LTR, and PD in univariable and multivariable analyses. Variables included in multivariable analyses included all variables significant in any individual univariable analysis: age, smoking status, histology, Eastern Cooperative Oncology Group (ECOG) performance status, dNLR, type of therapy (ICI monotherapy vs. dual ICI therapy), PD-L1, and TMB (**Fig. 2A–C**; Supplementary Fig. S6A–S6C). In multivariable analyses, TMB ≥ 50th percentile was independently associated with LTR compared with STR (adjusted OR, 2.74; 95% CI, 1.48–5.16, $P = 0.001$), as well as compared with non-LTR (adjusted OR, 2.57; 95% CI, 1.65–4.07; $P < 0.001$) and compared with PD (adjusted OR, 2.52; 95% CI, 1.55–4.18, $P < 0.001$). In contrast, whereas PD-L1 ≥ 50% was independently associated with LTR compared with non-LTR (adjusted OR, 3.76; 95% CI, 2.43–5.95, $P < 0.001$) and compared with PD (adjusted OR, 5.72; 95% CI, 3.54–9.44, $P < 0.001$) in multivariable analyses, PD-L1 ≥ 50% was not associated with LTR compared with STR in univariable (OR, 1.19; 95% CI, 0.76–1.87, $P = 0.488$) or multivariable analyses (adjusted OR, 1.55; 95% CI, 0.82–2.97, $P = 0.181$). Similarly, TMB ≥ 50th percentile ($P = 0.032$) associated

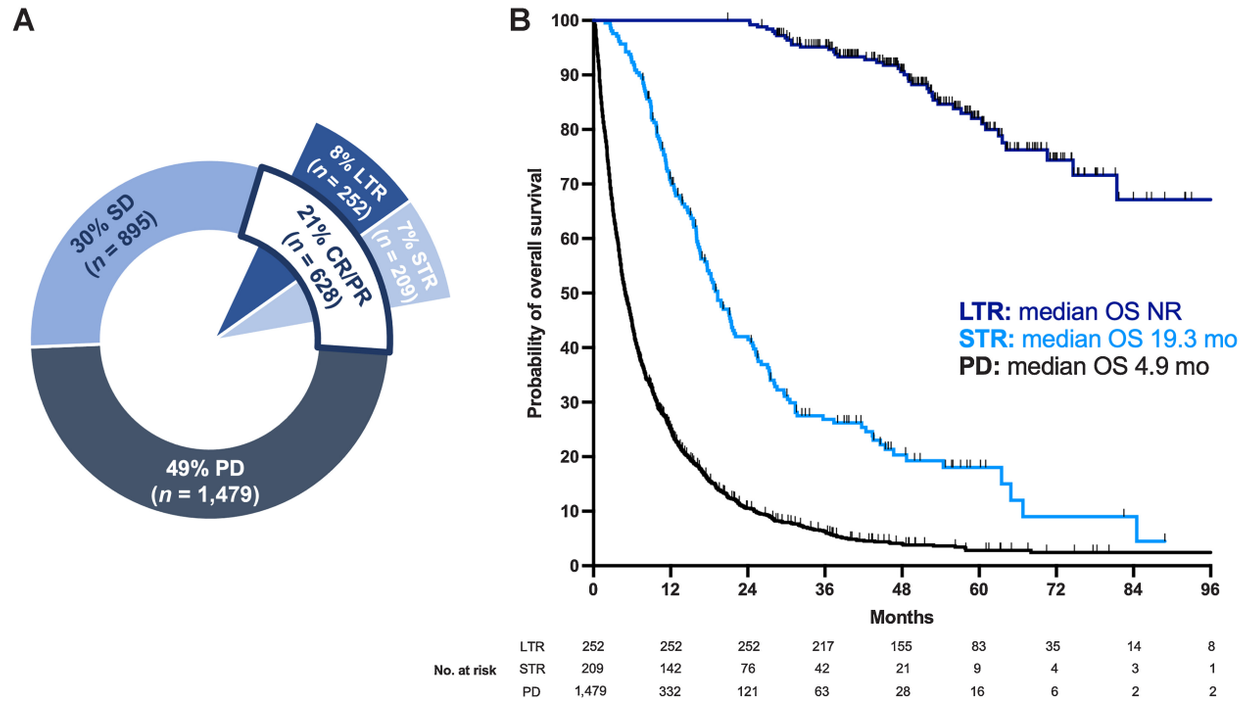

Figure 1.

Frequency and OS of patients with LTR, STR, and PD in the combined cohort. **A,** Number and percentage of patients in the combined cohort with BOR of PD, SD, CR/PR. The numbers and percentages of all patients achieving LTR and STR are displayed within the CR/PR subset. BOR information was not available for 116 patients (4%, not displayed). **B,** Kaplan–Meier curves of OS among LTR, STR, and PD patients in the combined cohort. Tick marks indicate censored data.

with CR compared with non-CR patients in multivariable analyses, whereas PD-L1 ≥ 50% did not ($P = 0.100$, Supplementary Fig. S7).

Additional clinical features of interest included squamous histology, which was negatively associated with LTR compared with STR in univariable (OR, 0.50; 95% CI, 0.30–0.82, $P = 0.010$; Supplementary Fig. S6A) and multivariable analyses (adjusted OR, 0.36; 95% CI, 0.13–0.93, $P = 0.040$; **Fig. 2A**). In addition, dNLR < 3.0 was associated with LTR compared with STR (OR, 1.98; 95% CI, 1.30–3.06, $P = 0.002$), LTR compared with non-LTR (OR, 2.00; 95% CI, 1.47–2.73, $P < 0.001$), and LTR compared with PD (OR, 2.55; 95% CI, 1.86–3.49, $P < 0.001$) in univariable analyses (Supplementary Fig. S6A–S6C), although not significant in any multivariable comparisons (**Fig. 2A–C**). Taken together, these analyses suggest high TMB and nonsquamous histology uniquely distinguish LTR compared with STR patients, and nominate dNLR as an additional candidate for further exploration.

PD-L1 and TMB among LTR and STR patients

Given the association of TMB ≥ 50th percentile but lack of association of PD-L1 ≥ 50% status with LTR compared with STR (**Fig. 3A** and **B**; Supplementary Fig. S8), we next asked whether higher TMB or PD-L1 cutoffs which have yet to reach routine clinical practice could either enrich or further enrich for LTR compared with STR. We explored two recently identified features associated with improved clinical benefit to ICI therapy in NSCLC: TMB ≥ 90th percentile (38) and PD-L1 ≥ 90% (39). In univariable and multivariable analyses, TMB ≥ 90th percentile (corresponding to TMB ≥ 19.7 mut/Mb for

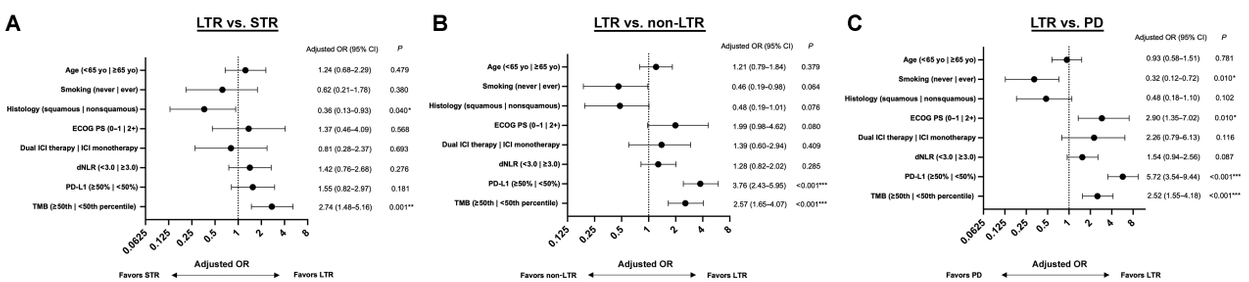

Figure 2.

Multivariable analyses of association of clinical characteristics with LTR compared with STR, non-LTR, and PD. Multivariable adjusted ORs and two-sided *P* values of association of clinical covariates with LTR compared with STR (**A**), LTR compared with non-LTR (**B**), and LTR compared with PD from multivariable logistic regression analyses (**C**) incorporating age, smoking status, histology, ECOG PS, type of therapy (dual ICI therapy versus ICI monotherapy), dNLR, PD-L1, and TMB. Dual ICI therapy = anti-PD-(L)1 therapy + anti-CTLA-4 therapy; ICI monotherapy = anti-PD-(L)1 monotherapy. *, $P < 0.05$; **, $P < 0.01$; ***, $P < 0.001$.

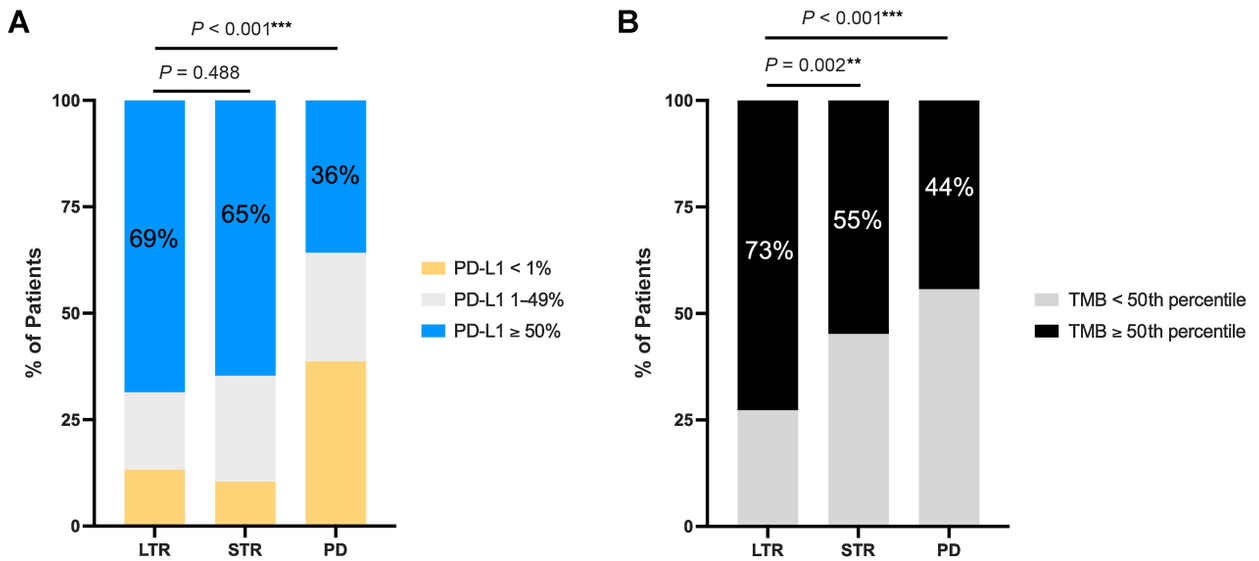

Figure 3.

Tumor PD-L1 expression distributions and TMB frequencies among patients with LTR, STR, and PD. **A,** Stacked bar graphs of percentage of patients with LTR, STR, and PD with PD-L1 < 1%, 1%–49%, and ≥ 50%. Two-sided *P* values from Fisher exact tests of associations of PD-L1 ≥ 50% with LTR compared with STR and LTR compared with PD are displayed. **B,** Bar graphs of percentage of patients with LTR, STR, and PD with TMB < 50th percentile and ≥ TMB 50th percentile in each cohort. Two-sided *P* values from Fisher exact tests of associations of TMB ≥ 50th percentile with LTR compared with STR and LTR compared with PD are displayed. **, $P < 0.01$; ***, $P < 0.001$.

MSK and ≥19.4 mut/Mb for DFCI) further enriched for LTR compared with STR in univariable (OR, 3.47; 95% CI, 1.74–6.99, $P < 0.001$) and multivariable (adjusted OR, 5.65; 95% CI, 2.13–18.1, $P = 0.001$) analyses. In contrast, PD-L1 ≥ 90% did not enrich for LTR compared with STR in univariable (OR, 0.98; 95% CI, 0.62–1.56, $P > 0.999$) or multivariable (adjusted OR, 0.71; 95% CI, 0.38–1.32, $P = 0.276$) analyses. Furthermore, when considering nonsquamous patients only (40), neither PD-L1 ≥ 50% (OR, 1.17; 95% CI, 0.72–1.89, $P = 0.611$; adjusted OR, 1.60; 95% CI, 0.80–3.21, $P = 0.186$) nor PD-L1 ≥ 90% (OR, 1.03; 95% CI, 0.63–1.67, $P > 0.999$; adjusted OR, 0.84; 95% CI, 0.44–1.63, $P = 0.610$) was associated with LTR compared with STR in univariable and multivariable analyses, respectively.

We also asked whether a composite of PD-L1 and TMB status could generally enrich for patients poised to achieve LTR. Interestingly, among patients with available PD-L1 and TMB information, we observed a >15 fold enrichment for achievement of LTR among patients with PD-L1 ≥ 50% and TMB ≥ 50th percentile (58/306, 19.0%) compared with patients with PD-L1 < 50% and TMB < 50th percentile (5/342, 1.5%; OR, 15.8; 95% CI, 6.6–36.9, $P < 0.001$; Supplementary Fig. S9). In addition, we observed that among 119 LTR patients with available TMB and PD-L1 information, 114 (96%) had either PD-L1 ≥ 50% or TMB ≥ 50th percentile, suggesting that at least one of these features is required for achievement of LTR in a vast majority of patients. However, it should be noted that 95 of 112 (85%) STR patients with available information had either PD-L1 ≥ 50% or TMB ≥ 50th percentile, suggesting limited ability of this combined metric to distinguish LTR from STR.

Association of depth of response with LTR and STR

We next examined baseline and on-treatment imaging characteristics associated with LTR. Patients with LTR had deeper median responses compared with STR among patients with available RECIST data (median BOR −65% vs. −46%, $P < 0.001$; **Fig. 4A**). In addition, a higher fraction of patients with LTR achieved a BOR of −50% or greater (72% vs. 40%; OR, 3.87; 95% CI, 2.39–6.27, $P < 0.001$) and −80% or greater (23% vs. 8%; OR, 3.39; 95% CI, 1.67–7.03, $P < 0.001$) compared with patients with STR. When stratifying patients by BOR status, we observed significant associations between BOR depth and LTR frequency. Patients with BOR of −30% to −49% achieved LTR in 45/140 cases (32%), patients with BOR of −50% to −79% achieved LTR in 76/133 cases (57%), and patients with BOR of −80% to −100% achieved LTR in 37/53 cases (70%; **Fig. 4B**). ORs for LTR among patients with BOR −50% to −79% and −80% to −100% compared with patients with BOR −30% to −49% were 2.82 (95% CI, 1.72–4.59, $P < 0.001$) and 4.88 (95% CI, 2.45–9.48, $P < 0.001$), respectively. The median baseline tumor burden (sum of RECIST target lesions at baseline) was not significantly different between patients with LTR and STR ($P = 0.459$) or LTR and PD ($P = 0.468$; **Fig. 4C**).

Genomic features of LTR and STR

We next sought to determine whether patients with LTR were specifically enriched for individual genomic features compared with patients with STR. Given significant association of nonsquamous histology with LTR and known genomic differences between nonsquamous and squamous NSCLC (41), we focused our analysis on oncogenic or likely oncogenic alterations in samples from nonsquamous patients only (1,450 total patients; MSK: 754, DFCI: 696; Supplementary Table S3). No alterations were significantly enriched among patients with LTR compared with STR (P_{adj} values for all genes > 0.05), although *ARID1A* (10% vs. 3%, $P = 0.036$) and *TP53* (72% vs. 59%, $P = 0.042$) alterations were numerically more frequent and *STK11* alterations (8% vs. 17%, $P = 0.028$) were numerically less frequent among LTR compared with STR (**Fig. 5A**). *EGFR* ($P < 0.001$, $P_{adj} = 0.004$) and *STK11* ($P < 0.001$, $P_{adj} = 0.006$) alterations were significantly underrepresented among LTR compared to PD (Supplementary Fig. S10A and S10B). Interestingly, when stratified by TMB

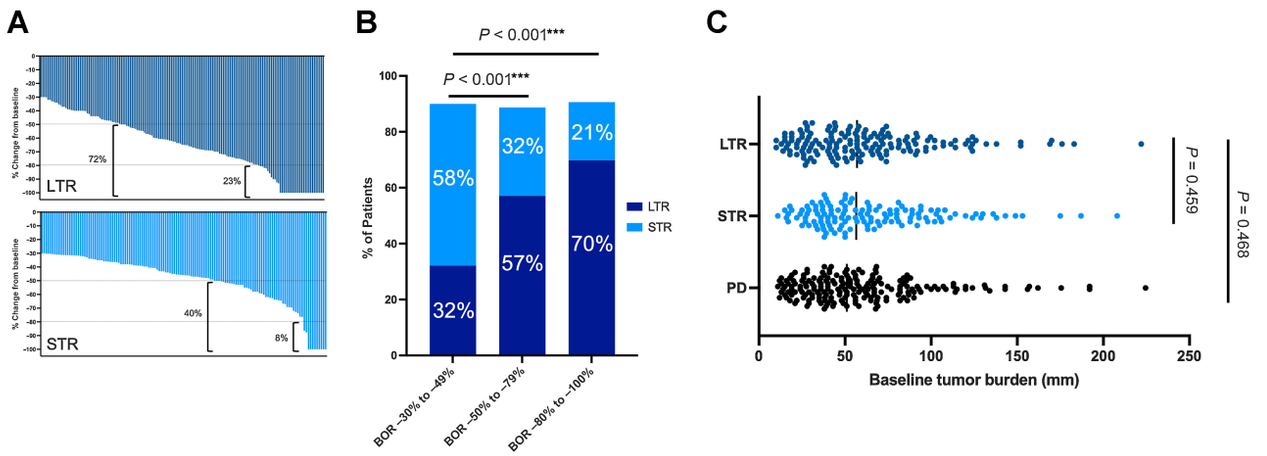

Figure 4.

Association of depth of response and baseline tumor burden with LTR and STR. **A,** Waterfall plots of BOR among patients with LTR and STR. Among patients with LTR, 72% achieved a BOR of −50% or greater and 23% achieved a BOR of −80% or greater. Among patients with STR, 40% achieved a BOR of −50% or greater and 8% achieved a BOR of −80% or greater. **B,** Frequency of LTR and STR among patients with a BOR of −30% to −49%, −50% to −79%, and −80% to −100%. Two-sided *P* values from Fisher exact tests for proportions of LTR between BOR categories are displayed. A subset of patients showed initial CR/PR but did not fall into LTR or STR categories; hence, proportions do not sum to 100%. **C,** Baseline tumor burden (sum of diameter of RECIST target lesions) among LTR, STR, and PD patients in the combined cohort. Two-sided *P* values for Mann–Whitney *U* tests comparing median tumor burden among patients with LTR versus STR and LTR versus PD are displayed. ***, $P < 0.001$.

status (Supplementary Figs. S11 and S12; Supplementary Table S4), the associations of *ARID1A* and *TP53* alterations with LTR compared with STR were lost, whereas trends toward association of *STK11* alterations with STR compared with LTR were retained (TMB-high subgroup: $P = 0.060$, TMB-low subgroup: $P = 0.077$). There were no significant differences among patients with LTR and STR with regard to fraction of genome altered ($P = 0.543$; Supplementary Fig. S13A), frequency of whole-genome doubling ($P = 0.365$; Supplementary Fig. S13B), HLA diversity (number of distinct HLA class I alleles, $P = 0.202$; Supplementary Fig. S13C), or frequency of HLA LOH ($P = 0.386$; Supplementary Fig. S13D).

We additionally performed WES and neoantigen prediction on samples from a subset of patients (28 LTR, 13 STR, and 42 PD; Supplementary Fig. S14A–S14F) in order to gain further insight into genomic features associated with LTR. Interestingly, among samples profiled by WES, both clonal (OR, 3.37; 95% CI, 1.23–15.6, $P = 0.061$)

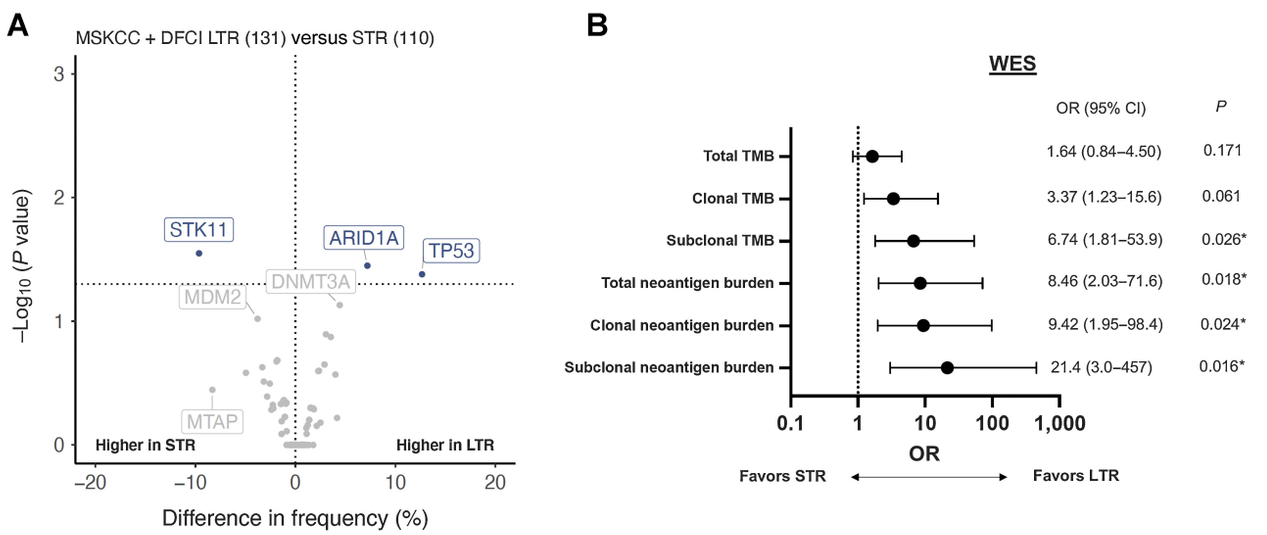

Figure 5.

Genomic features of patients with LTR compared with patients with STR. **A,** Volcano plot of genes with oncogenic or likely oncogenic alterations enriched among nonsquamous patients with LTR compared with patients with STR with available MSK-IMPACT or DFCI OncoPanel NGS. Plot depicts difference in frequency of individual gene alterations between LTR and STR (*x*-axis) versus $-\log_{10}$ (*P*) for Fisher exact test between LTR and STR groups (*y*-axis); horizontal dashed line corresponds to $P = 0.05$ cutoff. **B,** WES features of patients with LTR compared with STR. Displayed are univariable ORs and two-sided *P* values from logistic regression analyses of association between displayed covariates and binary outcome (LTR compared with STR). The lower and upper bounds of the 95% CI for ORs are shown as dots and whiskers. *, $P < 0.05$.

and subclonal TMB (OR, 6.74; 95% CI, 1.81–53.9, $P = 0.026$) distinguished LTR from STR (**Fig. 5B**). Correspondingly, TMB clonal architecture did not appear to be significantly different among LTR and STR, as no significant differences were found when comparing fraction of subclonal nonsynonymous mutations between patients with LTR and STR in general (Supplementary Fig. S15A) and when stratifying by total TMB status (Supplementary Fig. S15B and S15C). Similarly, both clonal and subclonal neoantigen burden distinguished LTR from STR (**Fig. 5B**).

Discussion

In this study, we describe the clinical, genomic, and pathologic features of, to our knowledge, the largest assembled series of long-term responders to ICI therapy in advanced NSCLC to date. We identified LTR (ongoing response ≥ 24 months) as an uncommon but profound clinical outcome in a subset of patients treated with ICIs, with LTR associated with a 5-year survival rate > 80% and > 50% of patients with LTR remaining progression-free at 5 years.

As has been previously suggested (21), we confirmed high TMB, independently evaluated through both NGS and WES, as a strong independent predictor of LTR compared with STR. Very high TMB, defined by TMB ≥ 90th percentile, even more strongly associated with LTR than TMB ≥ 50th percentile. The association of high TMB with LTR generally corresponds to a recent study demonstrating increased OS with ICI monotherapy among patients with advanced NSCLC with TMB ≥ 20 mut/Mb compared with patients with TMB 10 to 19 mut/Mb (22) and prior studies identifying TMB ≥ 90th percentile compared with TMB < 90 percentile as an optimal cutpoint for objective response and associated with improved OS to ICI therapy (38). In contrast, we show that high or very high PD-L1 (defined by PD-L1 ≥ 50% and ≥ 90%, respectively) does not independently distinguish LTR from STR. High PD-L1 may therefore not associate with durability of response, despite PD-L1 currently being the only approved histology-specific biomarker used to determine ICI eligibility in advanced NSCLC.

We also identify a number of key clinical features uniquely associated with LTR. In particular, we identify an independent enrichment for nonsquamous histology among LTR compared with STR, which was also recently demonstrated among durable responders to ICI therapy with or without chemotherapy (22) and may inform prognostication among patients with squamous histology treated with ICIs. In addition, we identify dNLR as a candidate predictive feature of LTR which warrants further exploration in larger studies, as low dNLR has recently been described as a feature of response and initial clinical benefit to ICI therapy in patients with NSCLC either independently (42–44) or in combination with high TMB (45). Finally, we identify strong links between depth of response and long-term durability of response to ICI therapy in NSCLC, which has recently also been demonstrated among patients receiving first-line ipilimumab and nivolumab (46) and in small cohorts of patients receiving ICI monotherapy (47, 48). These findings suggest that assessing depth of response, perhaps through more routine clinical approaches including assessment of circulating tumor DNA reduction or clearance (49, 50), may assist with prognostication of long-term outcomes among ICI-treated patients.

Beyond summary metrics, despite comprehensive genomic profiling of over 1,700 ICI-treated patients, no individual genomic features uniquely distinguished LTR from STR. Alterations in *ARID1A* have been linked to increased PD-L1 expression and TIL infiltration across solid tumors (51), with recent studies identifying associations of *ARID1A* alterations with prolonged PFS to ICIs across cancers (52), while *STK11* alterations are established markers of resistance to ICIs in *KRAS*-mutant NSCLC (53, 54). In our dataset, *ARID1A* and *TP53* alterations were more frequent among patients with LTR compared with STR. However, these associations were lost when stratifying for TMB status, further supportive of high TMB driving LTR among patients in our cohort. In contrast, the association of *STK11* alterations with non-LTR and PD, and trends toward association with STR compared with LTR appeared to be preserved independent of TMB status, suggesting that alternative mechanisms, such as impaired antigen processing and presentation (55), may contribute to the lack of LTR to ICIs observed among patients with advanced lung cancer and *STK11* alterations.

Our results also suggested that both clonal and subclonal TMB may be markers of LTR in advanced NSCLC. Further efforts are required to deepen our understanding of the relative contribution of individual nonsynonymous mutations, and the clonal architecture of these mutations, to durable response to ICIs. For example, recent efforts have uncovered strong contributions of "persistent" mutations present in single-copy regions or in multiple copies per cell (56), as well as limited numbers of immunodominant mutations irrespective of tumor mutational loads (57), on response to ICIs. Notably, where these mutations fall across the spectrum of clonal heterogeneity in different tumor types remains unclear (56) and should be explored in future studies.

The large size of our multicenter cohort, depth of clinical annotation, number of patients with NGS profiling, and inclusion of both clinical trial and standard of care patients all contribute to the strength and generalizability of our study. Our analyses suggest that while clinical features and TMB can assist with identifying subsets of patients poised to achieve LTR, pretreatment NGS profiling has limited further utility in identifying these patients. Our study may also serve as an initial step toward repositioning the role of TMB when deciding among systemic therapy options for patients with advanced NSCLC. Inclusion of TMB as a key stratification feature in future prospective studies evaluating the optimal length of ICI treatment among patients achieving a PFS of two years (58), or the efficacy of ICI monotherapy compared with combination ICI and chemotherapy among patients with high PD-L1, could further define the role of TMB in driving LTR to ICIs. Finally, given association of on-treatment radiographic responses with long-term outcomes observed in our study, it is likely that more dynamic profiling including pre and on-treatment evaluation of T-cell receptor dynamics, profiling of additional tumor microenvironment components, and/or transcriptomic-based approaches may also be needed to capture additional drivers of LTR (59).

In summary, we describe LTR as a relatively uncommon but profound clinical outcome in subsets of patients with advanced NSCLC treated with ICIs, identifying unique clinical and immunogenomic features, in particular, high TMB, associated with durable response to therapy. Importantly, features predicting long-term response may be distinct from those predicting initial response. Further work is needed to more comprehensively capture additional drivers of this remarkable clinical phenotype.

Authors' Disclosures

B. Ricciuti reports personal fees and other support from Regeneron, AstraZeneca, and Amgen and other support from Targeted Oncology outside the submitted work. H. Rizvi reports employment at AstraZeneca (which began subsequent to the completion of this work). A. Elkrief reports grants from Canadian Institutes of Health Research, Royal College of Physicians and Surgeons of Canada, and Cedar's Cancer Foundation during the conduct of the study. J. Luo reports grants and personal fees from Erasca; grants from Genentech, Kronos Bio, Novartis, and Revolution Medicines; and personal fees from AstraZeneca, Astellas, Blueprint Medicines, and

Daiichi Sankyo outside the submitted work; in addition, J. Luo has a patent for PCT/US2023/115872 filed by Memorial Sloan Kettering Cancer Center related to multimodal features to predict response to immunotherapy pending. J. Zhang reports grants and personal fees from Johnson and Johnson and Novartis; grants from Merck and Bristol Myers Squibb; and personal fees from AstraZeneca, GenePlus, Innovent, Hengrui, and Varian outside the submitted work. J.V. Heymach reports other support from Bristol-Myers Squibb; personal fees and other support from AstraZeneca, Boehringer-Ingelheim, Spectrum Pharmaceuticals, Mirati Therapeutics, and Takeda Pharmaceuticals; and personal fees from Genentech, Mirati Therapeutics, Eli Lilly & Co, Janssen Pharmaceuticals, Regeneron, BerGenBio, Jazz Pharmaceuticals, Curio Science, Novartis, BioAlta, Sanofi, GlaxoSmithKline, EMD Serono, BluePrint Medicine, and Chugai Pharmaceutical outside the submitted work. D.L. Gibbons reports grants and personal fees from AstraZeneca, Sanofi, and Astellas; personal fees from Menarini Recherche, Onconova, and Eli Lilly; and grants from Sanofi, Ribon Therapeutics, Janssen, Takeda, Boehringer Ingelheim, NGM Biopharmaceuticals outside the submitted work. C. Vanderbilt reports grants from Warren Alpert Foundation and other support from Paige AI outside the submitted work. M. Ladanyi reports personal fees from AstraZeneca outside the submitted work. C.M. Rudin reports personal fees from AbbVie, Amgen, AstraZeneca, Bristol Myers Squibb, Daiichi Sankyo, D2G Oncology, Genentech/Roche, Jazz, Lilly, Merck, Novartis, Bridge Medicines, and Harpoon Therapeutics and other support from Earli and Auron outside the submitted work. M.G. Kris reports personal fees and nonfinancial support from AstraZenaca and Genentech and personal fees from Merus, Pfizer, BerGenBio, Mirati, Daiichi Sankyo, Novartis, and Sanofi outside the submitted work. G.J. Riely reports grants from Mirati, Lilly, Takeda, Merck, Roche, Pfizer, Rain Therapeutics, and Novartis outside the submitted work. J.E. Chaft reports grants from NCI P30 CA008748 during the conduct of the study as well as personal fees from AstraZeneca, BMS, Genentech, Merck, Regeneron, Guardant Health, Arcus Bioscience, and Lilly outside the submitted work. M.D. Hellmann reports other support from AstraZeneca during the conduct of the study as well as other support from AstraZeneca outside the submitted work; in addition, M.D. Hellmann has a patent filed by MSK related to TMB as a biomarker of response to immunotherapy pending and licensed to PGDx. N.I. Vokes reports personal fees from Sanofi, OncoCyte, Eli Lilly, Regeneron, Amgen, and AstraZeneca outside the submitted work. M.M. Awad reports grants and personal fees from Bristol-Myers Squibb; personal fees from Merck, Pfizer, Gritstone, Foundation Medicine, Novartis, Mirati, EMD Serono, AstraZeneca, Instil Bio, Regeneron, Janssen, Affini-T; and grants from Amgen, Genentech, and Lilly during the conduct of the study. A.J. Schoenfeld reports grants and personal fees from BMS, Merck, Iovance Biotherapeutics, and Amgen; personal fees from Johnson & Johnson, KSQ Therapeutics, Enara Bio, Perceptive Advisors, Oppenheimer and Co, Umoja Biopharma, Legend Biotech, Prelude Therapeutics, Immunocore, Lyell Immunopharma, Heat Biologics; and grants from GSK, PACTpharma, Achilles Therapeutics, and Harpoon Therapeutics outside the submitted work. No disclosures were reported by the other authors.

Authors' Contributions

R. Thummalapalli: Conceptualization, data curation, formal analysis, funding acquisition, investigation, methodology, and writing–original draft. **B. Ricciuti:** Conceptualization, data curation, writing–review, and editing. **C. Bandlamudi:** Formal analysis, writing–review, and editing. **D. Muldoon:** Formal analysis, writing–review, and editing. **H. Rizvi:** Conceptualization and data curation. **A. Elkrief:** Data curation. **J. Luo:** Conceptualization, writing–review, and editing. **J.V. Alessi:** Data curation, writing–review, and editing. **F. Pecci:** Data curation. **G. Lamberti:** Data curation, writing–review, and editing. **A. Di Federico:** Data curation, writing–review, and editing. **L. Hong:** Data curation. **J. Zhang:** Data curation. **J.V. Heymach:** Resources, data curation, and supervision. **D.L. Gibbons:** Resources, data curation, and supervision. **A.J. Plodkowski:** Investigation and methodology. **V. Ravichandran:** Investigation and methodology. **M.T.A. Donoghue:** Investigation and methodology. **C. Vanderbilt:** Investigation and methodology. **M. Ladanyi:** Data curation, supervision, writing–review, and editing. **C.M. Rudin:** Resources, writing–review, and editing. **M.G. Kris:** Resources, writing–review, and editing. **G.J. Riely:** Conceptualization, resources, supervision, writing–review, and editing. **J.E. Chaft:** Supervision, writing–review, and editing. **M.D. Hellmann:** Conceptualization, resources, and supervision. **N.I. Vokes:** Conceptualization, resources, data curation, writing–review, and editing. **M.M. Awad:** Conceptualization, resources, supervision, writing–review, and editing. **A.J. Schoenfeld:** Conceptualization, resources, supervision, funding acquisition, writing–review, and editing.

Acknowledgments

The authors would like to thank Clare Wilhelm for his assistance with review and editing of this article. This work was supported by the NIH (cancer center grant P30 CA008748 to MSKCC, P30 CA016672 to MDACC, T32 CA009207 to R. Thummalapalli). This work was also supported by the generous philanthropic contributions to The University of Texas MD Anderson Lung Moon Shot Program. N.I. Vokes is supported by an ASCO Conquer Cancer Foundation Young Investigator Award, the SITC Genentech Women in Cancer Immunotherapy Fellowship, and the Mark Foundation Damon-Runyon Physician Scientist Training award. A.J. Schoenfeld is supported by an ASCO Career Development Award.

The publication costs of this article were defrayed in part by the payment of publication fees. Therefore, and solely to indicate this fact, this article is hereby marked "advertisement" in accordance with 18 USC section 1734.

Note

Supplementary data for this article are available at Clinical Cancer Research Online (http://clincancerres.aacrjournals.org/).

Received April 25, 2023; revised June 15, 2023; accepted July 7, 2023; published first July 11, 2023.

References

1. Reck M, Rodríguez-Abreu D, Robinson AG, Hui R, Csőszi T, Fülöp A, et al. Pembrolizumab versus chemotherapy for PD-L1–positive non–small-cell lung cancer. N Engl J Med 2016;375:1823–33.
2. Borghaei H, Paz-Ares L, Horn L, Spigel DR, Steins M, Ready NE, et al. Nivolumab versus docetaxel in advanced nonsquamous non–small-cell lung cancer. N Engl J Med 2015;373:1627–39.
3. Brahmer J, Reckamp KL, Baas P, Crinò L, Eberhardt WEE, Poddubskaya E, et al. Nivolumab versus docetaxel in advanced squamous-cell non–small-cell lung cancer. N Engl J Med 2015;373:123–35.
4. Herbst RS, Giaccone G, de Marinis F, Reinmuth N, Vergnenegre A, Barrios CH, et al. Atezolizumab for first-line treatment of PD-L1–selected patients with NSCLC. N Engl J Med 2020;383:1328–39.
5. Hellmann MD, Paz-Ares L, Bernabe Caro R, Zurawski B, Kim S-W, Carcereny Costa E, et al. Nivolumab plus Ipilimumab in advanced non–small-cell lung cancer. N Engl J Med 2019;381:2020–31.
6. Reck M, Rodríguez-Abreu D, Robinson AG, Hui R, Csőszi T, Fülöp A, et al. Five-year outcomes with pembrolizumab versus chemotherapy for metastatic non–small-cell lung cancer with PD-L1 tumor proportion score ≥ 50%. J Clin Oncol 2021;39:2339–49.
7. Garon EB, Hellmann MD, Rizvi NA, Carcereny E, Leighl NB, Ahn M-J, et al. Five-year overall survival for patients with advanced non–small-cell lung cancer treated with pembrolizumab: results from the phase I KEYNOTE-001 study. J Clin Oncol 2019;37:2518–27.
8. Schoenfeld AJ, Hellmann MD. Acquired resistance to immune checkpoint inhibitors. Cancer Cell 2020;37:443–55.
9. Heo JY, Yoo SH, Suh KJ, Kim SH, Kim YJ, Ock C-Y, et al. Clinical pattern of failure after a durable response to immune check inhibitors in non-small cell lung cancer patients. Sci Rep 2021;11:2514.
10. Schoenfeld AJ, Rizvi HA, Memon D, Shaverdian N, Bott MJ, Sauter JL, et al. Systemic and oligo-acquired resistance to PD-(L)1 blockade in lung cancer. Clin Cancer Res. 2022;28:3797–803.
11. Mok TSK, Wu Y-L, Kudaba I, Kowalski DM, Cho BC, Turna HZ, et al. Pembrolizumab versus chemotherapy for previously untreated, PD-L1-expressing, locally advanced or metastatic non-small-cell lung cancer (KEYNOTE-042): a randomised, open-label, controlled, phase 3 trial. Lancet 2019;393:1819–30.
12. Marcus L, Fashoyin-Aje LA, Donoghue M, Yuan M, Rodriguez L, Gallagher PS, et al. FDA approval summary: pembrolizumab for the treatment of tumor mutational burden-high solid tumors. Clin Cancer Res 2021;27:4685–9.
13. Hellmann MD, Nathanson T, Rizvi H, Creelan BC, Sanchez-Vega F, Ahuja A, et al. Genomic features of response to combination immunotherapy in patients with advanced non-small-cell lung cancer. Cancer Cell 2018;33:843–52.

14. Rizvi NA, Hellmann MD, Snyder A, Kvistborg P, Makarov V, Havel JJ, et al. Mutational landscape determines sensitivity to PD-1 blockade in non–small cell lung cancer. Science 2015;348:124–8.
15. Gandara DR, Paul SM, Kowanetz M, Schleifman E, Zou W, Li Y, et al. Blood-based tumor mutational burden as a predictor of clinical benefit in non-small-cell lung cancer patients treated with atezolizumab. Nat Med 2018;24:1441–8.
16. Hellmann MD, Ciuleanu T-E, Pluzanski A, Lee JS, Otterson GA, Audigier-Valette C, et al. Nivolumab plus ipilimumab in lung cancer with a high tumor mutational burden. N Engl J Med 2018;378:2093–104.
17. Rizvi H, Sanchez-Vega F, La K, Chatila W, Jonsson P, Halpenny D, et al. Molecular determinants of response to anti–programmed cell death (PD)-1 and anti–programmed death-ligand 1 (PD-L1) blockade in patients with non–small-cell lung cancer profiled with targeted next-generation sequencing. J Clin Oncol 2018;36:633–41.
18. Gataa I, Mezquita L, Rossoni C, Auclin E, Kossai M, Aboubakar F, et al. Tumour-infiltrating lymphocyte density is associated with favourable outcome in patients with advanced non-small cell lung cancer treated with immunotherapy. Eur J Cancer 2021;145:221–9.
19. Rakaee M, Adib E, Ricciuti B, Sholl LM, Shi W, Alessi JV, et al. Association of machine learning–based assessment of tumor-infiltrating lymphocytes on standard histologic images with outcomes of immunotherapy in patients with NSCLC. JAMA Oncol 2023;9:51–60.
20. Hu-Lieskovan S, Lisberg A, Zaretsky JM, Grogan TR, Rizvi H, Wells DK, et al. Tumor characteristics associated with benefit from pembrolizumab in advanced non-small cell lung cancer. Clin Cancer Res 2019;25:5061–8.
21. Frigola J, Navarro A, Carbonell C, Callejo A, Iranzo P, Cedrés S, et al. Molecular profiling of long-term responders to immune checkpoint inhibitors in advanced non-small cell lung cancer. Mol Oncol 2021;15:887–900.
22. Huang RSP, Carbone DP, Li G, Schrock A, Graf RP, Zhang L, et al. Durable responders in advanced NSCLC with elevated TMB and treated with 1L immune checkpoint inhibitor: a real-world outcomes analysis. J Immunother Cancer 2023;11:e005801.
23. Eisenhauer EA, Therasse P, Bogaerts J, Schwartz LH, Sargent D, Ford R, et al. New response evaluation criteria in solid tumours: revised RECIST guideline (version 1.1). Eur J Cancer 2009;45:228–47.
24. Cheng DT, Mitchell TN, Zehir A, Shah RH, Benayed R, Syed A, et al. Memorial sloan kettering-integrated mutation profiling of actionable cancer targets (MSK-IMPACT): a hybridization capture-based next-generation sequencing clinical assay for solid tumor molecular oncology. J Mol Diagn 2015;17:251–64.
25. Sholl LM, Do K, Shivdasani P, Cerami E, Dubuc AM, Kuo FC, et al. Institutional implementation of clinical tumor profiling on an unselected cancer population. JCI Insight 2016;1:e87062.
26. Garcia EP, Minkovsky A, Jia Y, Ducar MD, Shivdasani P, Gong X, et al. Validation of OncoPanel: a targeted next-generation sequencing assay for the detection of somatic variants in cancer. Arch Pathol Lab Med 2017;141:751–8.
27. Shen R, Seshan VE. FACETS: allele-specific copy number and clonal heterogeneity analysis tool for high-throughput DNA sequencing. Nucleic Acids Res 2016;44:e131.
28. Bielski CM, Zehir A, Penson AV, Donoghue MTA, Chatila W, Armenia J, et al. Genome doubling shapes the evolution and prognosis of advanced cancers. Nat Genet 2018;50:1189–95.
29. Shukla SA, Rooney MS, Rajasagi M, Tiao G, Dixon PM, Lawrence MS, et al. Comprehensive analysis of cancer-associated somatic mutations in class I HLA genes. Nat Biotechnol 2015;33:1152–8.
30. McGranahan N, Rosenthal R, Hiley CT, Rowan AJ, Watkins TBK, Wilson GA, et al. Allele-specific HLA loss and immune escape in lung cancer evolution. Cell 2017;171:1259–71.
31. AACR Project GENIE Consortium. AACR project GENIE: powering precision medicine through an international consortium. Cancer Discov 2017;7:818–31.
32. Vokes NI, Liu D, Ricciuti B, Jimenez-Aguilar E, Rizvi H, Dietlein F, et al. Harmonization of tumor mutational burden quantification and association with response to immune checkpoint blockade in non–small-cell lung cancer. JCO Precis Oncol 2019;3:PO.19.00171.
33. Chakravarty D, Gao J, Phillips SM, Kundra R, Zhang H, Wang J, et al. OncoKB: a precision oncology knowledge base. JCO Precis Oncol 2017;2017:PO.17.00011.
34. Cibulskis K, McKenna A, Fennell T, Banks E, DePristo M, Getz G, et al. ContEst: estimating cross-contamination of human samples in next-generation sequencing data. Bioinformatics 2011;27:2601–2.
35. Karczewski KJ, Francioli LC, Tiao G, Cummings BB, Alföldi J, Wang Q, et al. The mutational constraint spectrum quantified from variation in 141,456 humans. Nature 2020;581:434–43.
36. Bielski CM, Donoghue MTA, Gadiya M, Hanrahan AJ, Won HH, Chang MT, et al. Widespread selection for oncogenic mutant allele imbalance in cancer. Cancer Cell 2018;34:852–62.
37. Reynisson B, Alvarez B, Paul S, Peters B, Nielsen M. NetMHCpan-4.1 and NetMHCIIpan-4.0: improved predictions of MHC antigen presentation by concurrent motif deconvolution and integration of MS MHC eluted ligand data. Nucleic Acids Res 2020;48:W449–54.
38. Ricciuti B, Wang X, Alessi JV, Rizvi H, Mahadevan NR, Li YY, et al. Association of high tumor mutation burden in non–small cell lung cancers with increased immune infiltration and improved clinical outcomes of PD-L1 blockade across PD-L1 expression levels. JAMA Oncol 2022;8:1160–8.
39. Ricciuti B, Alessi JV, Alden S, Lamberti G, Vaz V, Barrichello A, et al. 312 Three-year outcomes with first-line pembrolizumab for metastatic non–small-cell lung cancer (NSCLC) with a very high PD-L1 tumor proportion score (TPS) ≥ 90%. J Immunother Cancer 2021;9.
40. Doroshow DB, Wei W, Gupta S, Zugazagoitia J, Robbins C, Adamson B, et al. Programmed death-ligand 1 tumor proportion score and overall survival from first-line pembrolizumab in patients with nonsquamous versus squamous NSCLC. J Thorac Oncol 2021;16:2139–43.
41. Heist RS, Sequist LV, Engelman JA. Genetic changes in squamous cell lung cancer: a review. J Thorac Oncol 2012;7:924–33.
42. Alessi JV, Ricciuti B, Alden SL, Bertram AA, Lin JJ, Sakhi M, et al. Low peripheral blood derived neutrophil-to-lymphocyte ratio (dNLR) is associated with increased tumor T-cell infiltration and favorable outcomes to first-line pembrolizumab in non-small cell lung cancer. J Immunother Cancer 2021;9:e003536.
43. Hwang M, Canzoniero JV, Rosner S, Zhang G, White JR, Belcaid Z, et al. Peripheral blood immune cell dynamics reflect antitumor immune responses and predict clinical response to immunotherapy. J Immunother Cancer 2022;10:e004688.
44. Mezquita L, Preeshagul I, Auclin E, Saravia D, Hendriks L, Rizvi H, et al. Predicting immunotherapy outcomes under therapy in patients with advanced NSCLC using dNLR and its early dynamics. Eur J Cancer 2021;151:211–20.
45. Valero C, Lee M, Hoen D, Weiss K, Kelly DW, Adusumilli PS, et al. Pretreatment neutrophil-to-lymphocyte ratio and mutational burden as biomarkers of tumor response to immune checkpoint inhibitors. Nat Commun 2021;12:729.
46. Borghaei H, Ciuleanu T-E, Lee J-S, Pluzanski A, Caro RB, Gutierrez M, et al. Long-term survival with first-line nivolumab plus ipilimumab in patients with advanced non-small cell lung cancer: a pooled analysis. Ann Oncol 2022;34:173–85.
47. McCoach CE, Blumenthal GM, Zhang L, Myers A, Tang S, Sridhara R, et al. Exploratory analysis of the association of depth of response and survival in patients with metastatic non-small-cell lung cancer treated with a targeted therapy or immunotherapy. Ann Oncol 2017;28:2707–14.
48. Jo H, Yoshida T, Yagishita S, Ohuchi M, Matsumoto Y, Shinno Y, et al. Clinical characteristics and pharmacokinetics change of long-term responders to anti-PD-1 inhibitor among patients with advanced non-small-cell lung cancer. JTO Clin. Res. Rep. 2023;4:100474.
49. Zou W, Yaung SJ, Fuhlbrück F, Ballinger M, Peters E, Palma JF, et al. ctDNA predicts overall survival in patients with NSCLC treated with PD-L1 blockade or with chemotherapy. JCO Precis Oncol 2021;5:827–38.
50. Raja R, Kuziora M, Brohawn PZ, Higgs BW, Gupta A, Dennis PA, et al. Early reduction in ctDNA predicts survival in patients with lung and bladder cancer treated with durvalumab. Clin Cancer Res 2018;24:6212–22.
51. Shen J, Ju Z, Zhao W, Wang L, Peng Y, Ge Z, et al. ARID1A deficiency promotes mutability and potentiates therapeutic antitumor immunity unleashed by immune checkpoint blockade. Nat Med 2018;24:556–62.
52. Okamura R, Kato S, Lee S, Jimenez RE, Sicklick JK, Kurzrock R. ARID1A alterations function as a biomarker for longer progression-free survival after anti-PD-1/PD-L1 immunotherapy. J Immunother Cancer 2020;8:e000438.
53. Skoulidis F, Goldberg ME, Greenawalt DM, Hellmann MD, Awad MM, Gainor JF, et al. STK11/LKB1 mutations and PD-1 inhibitor resistance in KRAS-mutant lung adenocarcinoma. Cancer Discov 2018;8:822–35.
54. Ricciuti B, Arbour KC, Lin JJ, Vajdi A, Vokes N, Hong L, et al. Diminished efficacy of programmed death-(Ligand)1 inhibition in STK11- and KEAP1-mutant lung adenocarcinoma is affected by KRAS mutation status. J Thorac Oncol 2022;17:399–410.
55. Deng J, Thennavan A, Dolgalev I, Chen T, Li J, Marzio A, et al. ULK1 inhibition overcomes compromised antigen presentation and restores antitumor immunity in LKB1-mutant lung cancer. Nat Cancer 2021;2:503–14.

56. Niknafs N, Balan A, Cherry C, Hummelink K, Monkhorst K, Shao XM, et al. Persistent mutation burden drives sustained anti-tumor immune responses. Nat Med 2023;29:440–9.
57. Puig-Saus C, Sennino B, Peng S, Wang CL, Pan Z, Yuen B, et al. Neoantigen-targeted CD8+ T cell responses with PD-1 blockade therapy. Nature 2023;615:697–704.
58. Sun L, Bleiberg B, Hwang W-T, Marmarelis ME, Langer CJ, Singh A, et al. Association between duration of immunotherapy and overall survival in advanced non–small cell lung cancer. JAMA Oncol 2023;e231891.
59. Davis-Marcisak EF, Deshpande A, Stein-O'Brien GL, Ho WJ, Laheru D, Jaffee EM, et al. From bench to bedside: Single-cell analysis for cancer immunotherapy. Cancer Cell 2021;39:1062–80.